A FOCUS ON MIXED-PHASE CLOUDS

The Status of Ground-Based Observational Methods

BY MATTHEW D. SHUPE, JOHN S. DANIEL, GIJS DE BOER, EDWIN W. ELORANTA, PAVLOS KOLLIAS, CHARLES N. LONG, EDWARD P. LUKE, DAVID D. TURNER, AND JOHANNES VERLINDE

Ground-based observational methods provide key insights into mixed-phase cloud macrophysical, microphysical, radiative, and dynamical properties, although significant deficiencies still exist.

The atmospheric radiation balance and hydrological cycle are intimately tied to clouds, and are particularly sensitive to the partitioning of cloud phase. Hydrometeors in liquid and ice phases typically occur in different sizes and shapes, nucleate under distinct conditions, grow and evaporate at differing rates, and fall at unique speeds (e.g., Pruppacher and Klett 1978). All of these properties profoundly impact the total cross-sectional and surface areas of hydrometeors in each phase, influencing their interaction with atmospheric radiation and the efficiency with which they grow to precipitation sizes.

The complex, three-way interaction between vapor, liquid, and ice in one cloud system that is unique to mixed-phase clouds[1] makes their structure and phase partitioning particularly difficult, yet important, to model correctly (Sun and Shine 1994; Gregory and Morris 1996). Recent observations have documented mixed-phase clouds in all seasons, under a variety of conditions, and in many locations worldwide. A great deal of focus has been on Arctic mixed-phase cloud observations (Rangno and Hobbs 1991; Pinto 1998; Hobbs and Rangno 1998; Turner 2005; Zuidema et al.

AFFILIATIONS: SHUPE—Cooperative Institute for Research in Environmental Science, and NOAA/Earth Science Research Laboratory, Boulder, Colorado; DANIEL—NOAA/Earth Science Research Laboratory, Boulder, Colorado; DE BOER AND ELORANTA—University of Wisconsin—Madison, Madison, Wisconsin; KOLLIAS AND LUKE—Brookhaven National Laboratory, Upton, New York; LONG—Pacific Northwest National Laboratory, Richland, Washington; TURNER—Space Science and Engineering Center, University of Wisconsin—Madison, Madison, Wisconsin; VERLINDE—The Pennsylvania State University, University Park, Pennsylvania
CORRESPONDING AUTHOR: Matthew Shupe, R/PSD3, 325 Broadway, Boulder, CO 80305
E-mail: matthew.shupe@noaa.gov

The abstract for this article can be found in this issue, following the table of contents.
DOI:10.1175/2008BAMS2378.1

In final form 28 April 2008

[1] Here we define *mixed-phase cloud* as a complete cloud system that contains both liquid and ice water in the vertical that interact via microphysical processes. While it is not necessary that all volumes in this system contain both phases, typically the system does contain some truly mixed-phase volumes. For example, in a case where ice crystals form in, and then fall out of, a supercooled liquid water cloud, both the liquid and ice regions are considered to be part of the mixed-phase system.

2005). One study has indicated that mixed-phase clouds occur approximately 40% of the time in the western Arctic, most frequently during the spring and fall transition seasons, and with a significant presence in the cold and dark Arctic winter (Shupe et al. 2006). In addition to the Arctic, mixed-phase clouds have been observed in Europe (Hogan et al. 2003a; Field et al. 2004), North America (Hobbs and Atkinson 1976; Rauber 1987; Heymsfield et al. 1991; Fleishauer et al. 2002), Australia (Platt 1977), Antarctica (Lubin 2004), and Asia (Gayet et al. 2002). Multiphase conditions are associated with frontal systems (Matejka et al. 1980; Hogan et al. 2002; Korolev et al. 2003), orography (Hobbs and Atkinson 1976; Rauber 1987; Heymsfield and Miloshevich 1993), and air masses containing African dust (Shupe et al. 2004), among other conditions. In addition to their climatic significance, supercooled liquid water in mixed-phase clouds is responsible for hazardous aircraft icing (e.g., Cober et al. 2001).

To properly model these clouds, further observational information is needed regarding the condensed mass and characteristic particle sizes of hydrometeors in both liquid and ice phases. For this reason, we assess the state-of-the-art, surface-based measurements and methods for characterizing mixed-phase cloud macrophysical, microphysical, radiative, and dynamical properties. The discussion here employs examples of single-layer Arctic stratiform mixed-phase clouds, which are one of the simplest mixed-phase cloud forms. Mixed-phase conditions associated with either deep convection or the melting of frozen precipitation are not considered here.

All observations used in this assessment were made during the Mixed-Phase Arctic Clouds Experiment (MPACE; Verlinde et al. 2007), which took place during autumn 2004 at the Department of Energy (DOE) Atmospheric Radiation Measurement (ARM) Program's North Slope of Alaska (NSA) site in Barrow, Alaska. Verlinde et al. (2007) describe the synoptic conditions under which these observations were obtained. The NSA is well equipped with instruments to measure most climatologically important parameters of the atmospheric radiation system and is similar to other atmospheric observatories (Ackerman and Stokes 2003; Haeffelin et al. 2005; Illingworth et al. 2007). Instruments deployed during MPACE that are used in the identification and/or characterization of mixed-phase cloud macrophysical, microphysical, radiative, and dynamical properties are summarized in Table 1, while example mixed-phase cloud measurements are displayed in Fig. 1. These include time–height measurements from cloud radar and lidar, and time series measurements of either atmospheric brightness temperatures or fluxes from a dual-channel microwave radiometer (MWR),

Table 1. Instruments for observing mixed-phase cloud properties during MPACE at the ARM North Slope of Alaska site in Barrow, Alaska.

Instrument	Specifications	Measurements	Reference
Millimeter Cloud Radar (MMCR)	Frequency: 35 GHz, wavelength: 8 mm, resolution: 45 m 4 s	Doppler spectrum, reflectivity, mean Doppler velocity, Doppler spectrum width	Moran et al. (1998) Kollias et al. (2007)
HSRL*	Wavelength: 532 nm, resolution: 5+ m, 2+ s	Backscatter, depolarization ratio	Eloranta (2005)
Micropulse Lidar (MPL)	Wavelength: 523 nm, resolution: 30 m, <30 s	Backscatter, depolarization ratio	Campbell et al. (2002)
Ceilometer	Wavelength: 905 nm, resolution: 15 m	Cloud-base height	—
AERI	Wavelength: 3300–400 cm^{-1} 3–25 μm, resolution: 1 cm^{-1} 30 s	Spectral radiance	Knutseon et al. (2004a,b)
Dual-channel MWR	Frequency: 23.8 GHz, 31.4 GHz, resolution: ~30 s	Brightness temperature	Liljegren (1994)
Near-IR spectrometer*	Wavelength: 0.9–1.7 μm, resolution: 4–5 nm 2 s	Spectral radiance	Daniel et al. (2006)
Broadband radiometers	Wavelength: 0.3–3 μm (SW), 4–50 μm (LW), resolution: 1 min	SW and LW flux	Barnard and Long (2004)
Radiosonde	Variable time and height resolution	Temperature, wind, relative humidity	—

* Guest instruments during the MPACE intensive observation period.

the Atmospheric Emitted Radiance Interferometer (AERI), and broadband shortwave (SW) and longwave (LW) radiometers [please refer to Verlinde et al. (2007) for a general description of the NSA instrumentation].

THE STATE OF OUR ABILITIES. Specific cloud retrieval methods for characterizing mixed-phase clouds are only briefly discussed here for the purpose of illustrating our present abilities. The reader is encouraged to pursue further details regarding the application and implementation of individual methods in the provided references. A summary of the pertinent cloud properties, their associated retrieval methods, and the conditions under which they are applicable is given in Table 2.

Macrophysics and phase. Perhaps the most successful aspect of the mixed-phase cloud characterization is of the macrophysical properties, including the presence and vertical location of cloud layers of different phases. Active sensing by cloud radar and lidar provides robust and consistent measurements of cloud boundaries in most cases. In addition, the combination of active and passive sensors at multiple wavelengths yields a strong constraint on cloud phase and its vertical distribution, which is an important precursor to applying further cloud property retrievals.

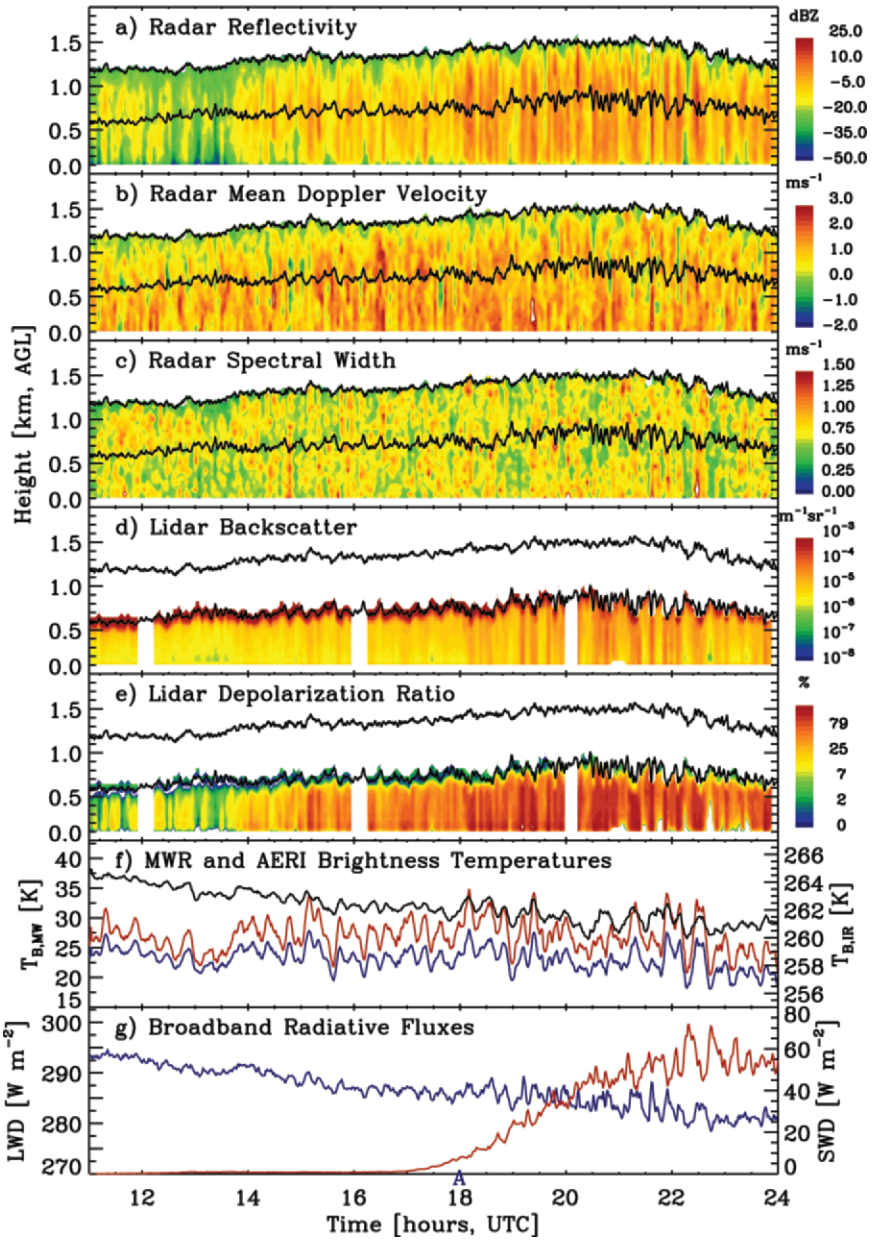

FIG. 1. Measurements from 9 Oct 2004 at Barrow of (a) radar reflectivity, (b) mean Doppler velocity, (c) Doppler spectrum width, (d) lidar backscatter cross section, (e) depolarization ratio, (f) microwave radiometer brightness temperatures at 23.8 (blue) and 31.4 (red) GHz and an infrared brightness temperature at 900 cm^{-1} from AERI (black, right ordinate), and (g) broadband longwave (blue, left ordinate) and shortwave (red, right ordinate) radiation. In (a)–(c) the cloud liquid base and top heights, from ceilometer and radar, respectively, are included.

Two classifications are highlighted here. The first is a fixed-constraint, multisensor approach, which exploits phase-specific signatures from radar, lidar, MWR, and radiosonde measurements to discriminate between phases (Shupe 2007). For example, mixed-phase conditions usually require a subfreezing temperature, a positive liquid water path (LWP), a region of low lidar depolarization ratio (<0.1), which indicates the presence of liquid water droplets, and a region of high radar reflectivity (>−17 dBZ), which indicates the presence of large ice particles. The

second classification method is based solely on measurements of the radar Doppler spectrum and uses a trained neural network that associates cloud type and phase with unique spectral signatures, such as bimodalities and spectral skewness (Luke and Kollias 2007). Both methods identify single-layer Arctic mixed phase stratiform clouds to be topped by a region of cloud liquid, within which ice crystals form and fall, and an underlying layer of falling ice-phase hydrometeors (Figs. 2a,b, and 4c). Remarkably, the

Table 2. Mixed-phase cloud properties, instruments used in their derivation, references for pertinent retrieval methods applied to mixed-phase clouds, and the conditions under which retrievals are applicable. SZA is the solar zenith angle.

Property	Instrument	Method	Conditions
Location, boundaries, thickness, persistence	Radar, lidar, ceilometer	Clothiaux et al. (2000)	All
Phase identification	Radar–lidar–MWR–radiosonde	Shupe (2007)	All
	Doppler radar spectra	Luke and Kollias (2007)	All
Ice water content/path	Radar	Shupe et al. (2006)	Ice-containing clouds
		Matrosov et al. (2002)	
	Lidar–radar	Donovan and van Lammeren (2001)	Nonocculted, all-ice cloud volumes
		Wang and Sassen (2002)	
		Hogan et al. (2003a, 2006)	
	AERI	Turner (2005)	$\tau < 6$, ice-containing clouds
	Near-IR	Daniel et al. (2006)	SZA ~<80°, ice-containing clouds
Ice particle size	Radar	Shupe et al. (2006)	Ice-containing clouds
	Lidar–radar	Donovan and van Lammeren (2001)	Nonocculted, all-ice cloud volumes
		Wang and Sassen (2002)	
		Hogan et al. (2003a, 2006)	
	AERI	Turner (2005)	$\tau < 6$, ice-containing clouds
Liquid water content	Radiosonde, adiabatic	Zuidema et al. (2005)	Stratiform, liquid-containing clouds
	Doppler radar spectra	Shupe et al. (2004)	Mixed-phase cases with bimodal Doppler spectra
		Verlinde et al. (2007)	
Liquid water path	MWR	Liljegren et al. (2001)	Liquid-containing cloud scenes, except rain
		Turner et al. (2007)	
	AERI	Turner (2005, 2007)	LWP <50 g m^{-2}, liquid-containing clouds
		Wang et al. (2004)	
	Near-IR	Daniel et al. (2006)	SZA ~<80°, liquid-containing clouds
	Radiosonde, adiabatic	Zuidema et al. (2005)	Stratiform, liquid-containing clouds
Liquid droplet radius	AERI	Turner (2005)	LWP <50 g m^{-2}, liquid-containing clouds
		Turner and Holz (2005)	
		Wang et al. (2004)	
	Doppler radar spectra	Shupe et al. (2004)	Mixed-phase cases with bimodal Doppler spectra
		Verlinde et al. (2007)	
Optical depth, liquid	AERI	Turner (2005)	LWP <50 g m^{-2}, liquid-containing clouds
	Near-IR	Daniel et al. (2006)	SZA ~<80°, liquid-containing clouds
		Portmann et al. (2001)	
	SW broadband	Bernard and Long (2004)	SZA <80°, liquid-containing clouds
	Radiosonde, adiabatic	$\tau = 1.5\ \mathrm{LWP}\ R_e^{-1}$	Stratiform, liquid-containing clouds
Optical depth, ice	AERI	Turner (2005)	$\tau < 6$, ice-containing clouds
	Radar	Matrosov et al. (2003)	Ice-containing clouds
		Hogan et al. (2003b)	
Optical depth, total	Lidar	Eloranta (2005)	Nonocculted cloud volumes
	AERI	Turner (2005)	$\tau < 6$, LWP < 50 g m^{-2}
Vertical velocity	Doppler radar spectra	Shupe et al. (2004, 2008b)	Liquid-containing cloud volumes
Turbulent dissipation rate	Radar	Shupe et al. (2008b)	All

Doppler radar spectra-only method (Fig. 2b) is able to accurately distinguish the base of the cloud liquid in spite of the dominant response of radar reflectivity to the larger ice particles in mixed-phase clouds (Figs. 1a and 5c).

Cloud ice microphysics. Mixed-phase cloud microphysical characterization is somewhat more difficult, but a number of retrieval methods exist for estimating some of these parameters. Vertical profiles and layer-averaged ice particle effective radius (R_{ei}) and ice water content (IWC) can be obtained from a combination of sources, including radar, lidar, IR, and near-IR measurements. Radar-based retrievals are most widely applicable because the radar senses the full, vertically resolved cloud column and because the radar signal responds to particle size to the sixth power, making it particularly useful for sensing relatively large ice crystals. This class of retrieval can be based on simple radar reflectivity power-law relations that have been tuned to a specific region (Shupe et al. 2006) or reflectivity Doppler velocity retrievals that capitalize on relationships between fall speed and particle size (Matrosov et al. 2002; Mace et al. 2002). Because lidar and radar signals are proportional to different powers of the particle size distribution, the ratio of lidar-to-radar backscatter cross sections is another means for deriving profiles of ice properties throughout the cloud depth observed by lidar (Donovan and van Lammeren 2001), which is prone to occultation. Lidar–radar methods are particularly useful in the optically thinner clouds that allow for full lidar penetration.

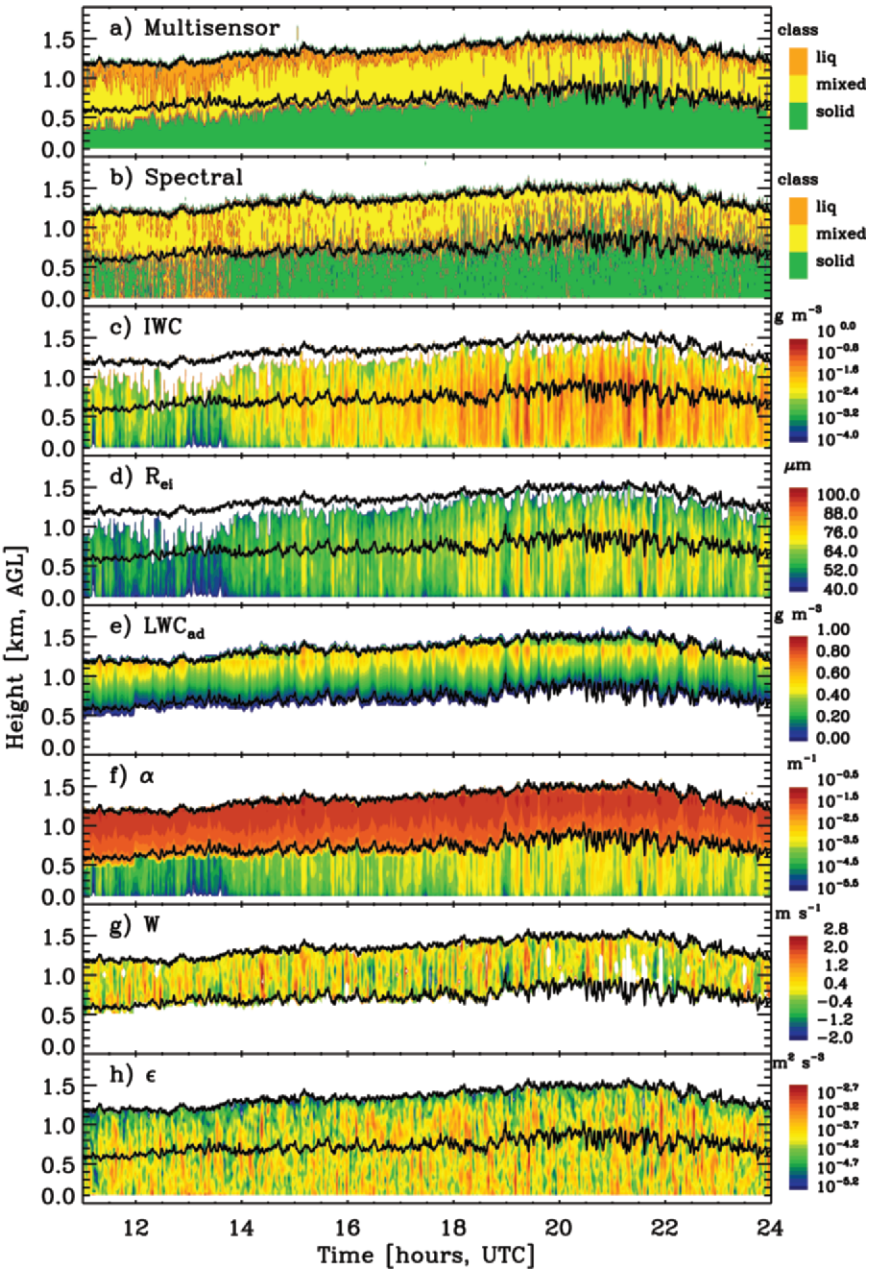

Fig. 2. Retrieved, vertically resolved cloud properties for 9 Oct 2004 at Barrow: (a) multisensor cloud phase classification, (b) Doppler radar spectra cloud phase classification, (c) ice water content derived from radar, (d) ice particle effective radius derived from radar, (e) adiabatic liquid water content derived from radiosonde temperature profiles, lidar cloud base, radar cloud top, and scaled to the microwave radiometer–derived liquid water path, (f) extinction derived from a combination of adiabatic liquid water properties and radar and lidar ice extinction, (g) vertical wind velocity derived from Doppler radar spectra (positive values are upward), and (h) turbulent dissipation rate derived from Doppler radar velocity. In each panel, the cloud liquid base and top from ceilometer and radar, respectively, are included.

Radiatively constrained ice property retrievals are available under certain conditions. Near-IR wavelengths can be exploited to derive IWP during daylight hours. Daniel et al. (2006) utilize scattered sunlight between 0.9 and 1.7 μm to compute a path-integrated ice water path (IWP), which represents the amount of ice encountered by photons that are scattered through the cloud layer and can be related to a vertically normalized IWP using assumptions about cloud micro- and macrophysical properties. For optically thin clouds (LWP <50 g m^{-2} or optical depth τ < 6), IR microwindows between 800–1200 and 400–600 cm^{-1} observed by AERI are semitransparent and contain information on cloud particles, which can be exploited to provide a layer-averaged ice particle size (Turner 2005).

Selected examples of these ice retrievals (Figs. 2c,d, 3c, and 4c) reveal the high variability of ice microphysical properties that is often found in Arctic stratiform mixed-phase cloud layers. One signature feature of these clouds is the pulse-like, or streaky, behavior of the cloud ice, which largely results from cloud-scale dynamics leading to pockets of ice formation or enhancement. Figure 3c shows IWP varying in pulses by more than 300 g m^{-2} over the course of 5 min. In the vertical, IWC profiles

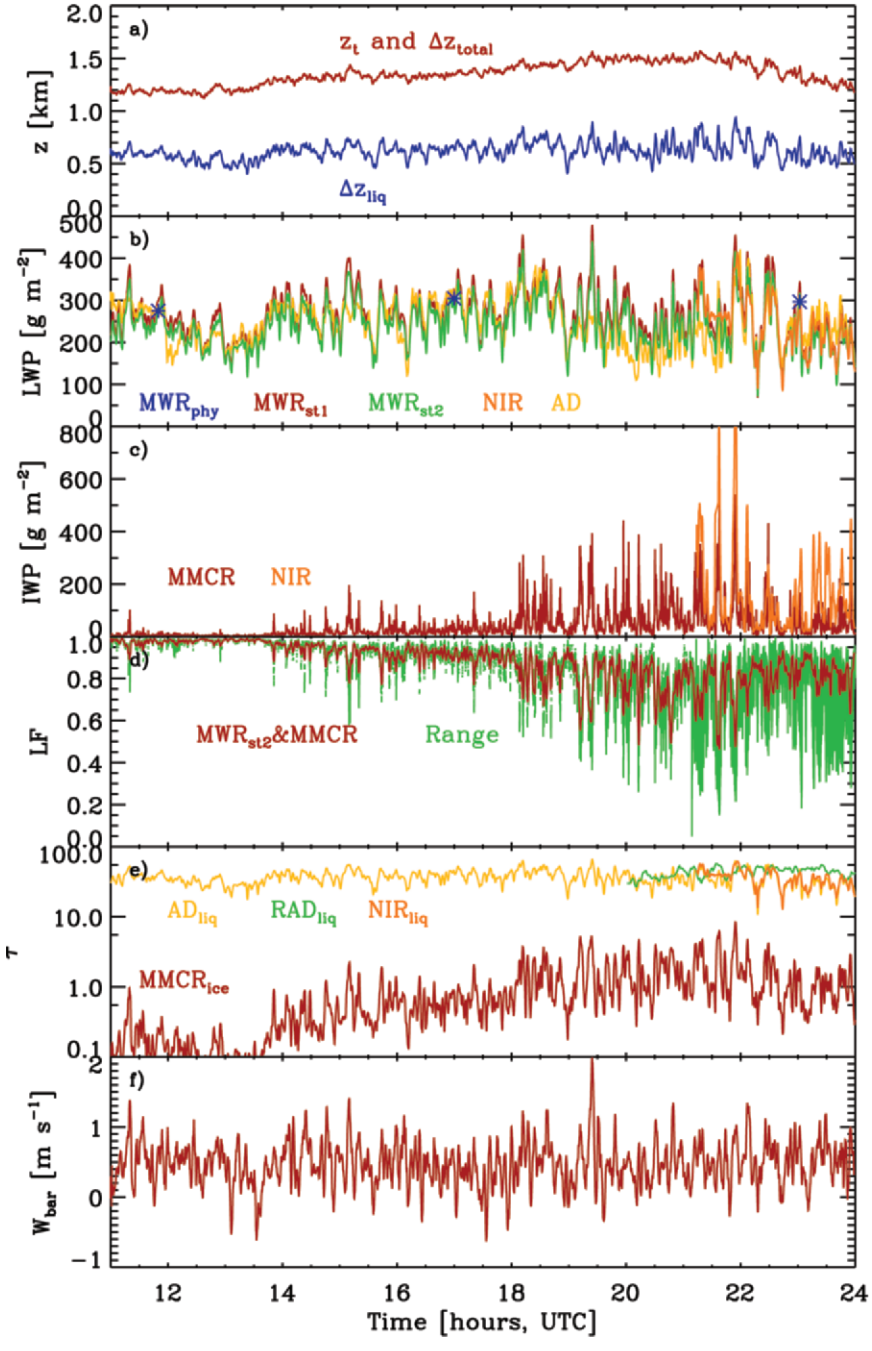

Fig. 3. Retrieved time series cloud properties for 9 Oct 2004: (a) cloud-top height and total (liquid + ice) cloud thickness (red) and liquid layer thickness (blue); (b) liquid water path derived from the microwave radiometer physical and two statistical retrievals, near-IR measurements, and an adiabatic assumption; (c) ice water path from radar and near-IR measurements; (d) the liquid fraction, defined as the ratio of liquid water path to total condensed water path, given as the range from all measurements (green) and a possible best estimate (red); (e) optical depth of cloud ice from the radar and cloud liquid from the near-IR, shortwave radiation, and adiabatic assumption; and (f) layer-mean vertical wind velocity from Doppler radar spectra (positive values are upward). The physical microwave LWP retrieval is only performed at sounding times. In (e), both the near-IR and adiabatic cloud liquid optical depths are derived assuming a droplet effective radius of 10 μm. All near-IR retrievals were limited to times of instrument operation and daylight, and the broadband radiometric optical depth retrieval requires a minimum solar zenith angle.

reveal the characteristic manner in which the ice grows throughout the cloud liquid layer but decreases below the liquid cloud base (e.g., Shupe et al. 2006, 2008a). Although there is reasonable agreement between these methods in terms of variability (the correlation coefficient for IWP in Fig. 3c is 0.67), the magnitude of differences between retrieval methods suggests uncertainties on the order of a factor of 2, which is in agreement with other uncertainty estimates based on comparisons with aircraft in situ observations (e.g., Matrosov et al. 2002; Shupe et al. 2005). Ice particle size retrieval comparisons (Fig. 4d) sometimes suffer from inconsistencies in the way each instrument observes the particles. For example, the AERI estimate of R_{ei} is substantially smaller than the radar estimate, likely because AERI retrievals may treat individual elements of an ice crystal (i.e., individual bullets of a bullet rosette) as distinct particles (Turner 2005). The High Spectral Resolution Lidar (HSRL)-based size estimate does not distinguish between phase, and thus falls between those sizes estimated for the liquid and ice particles.

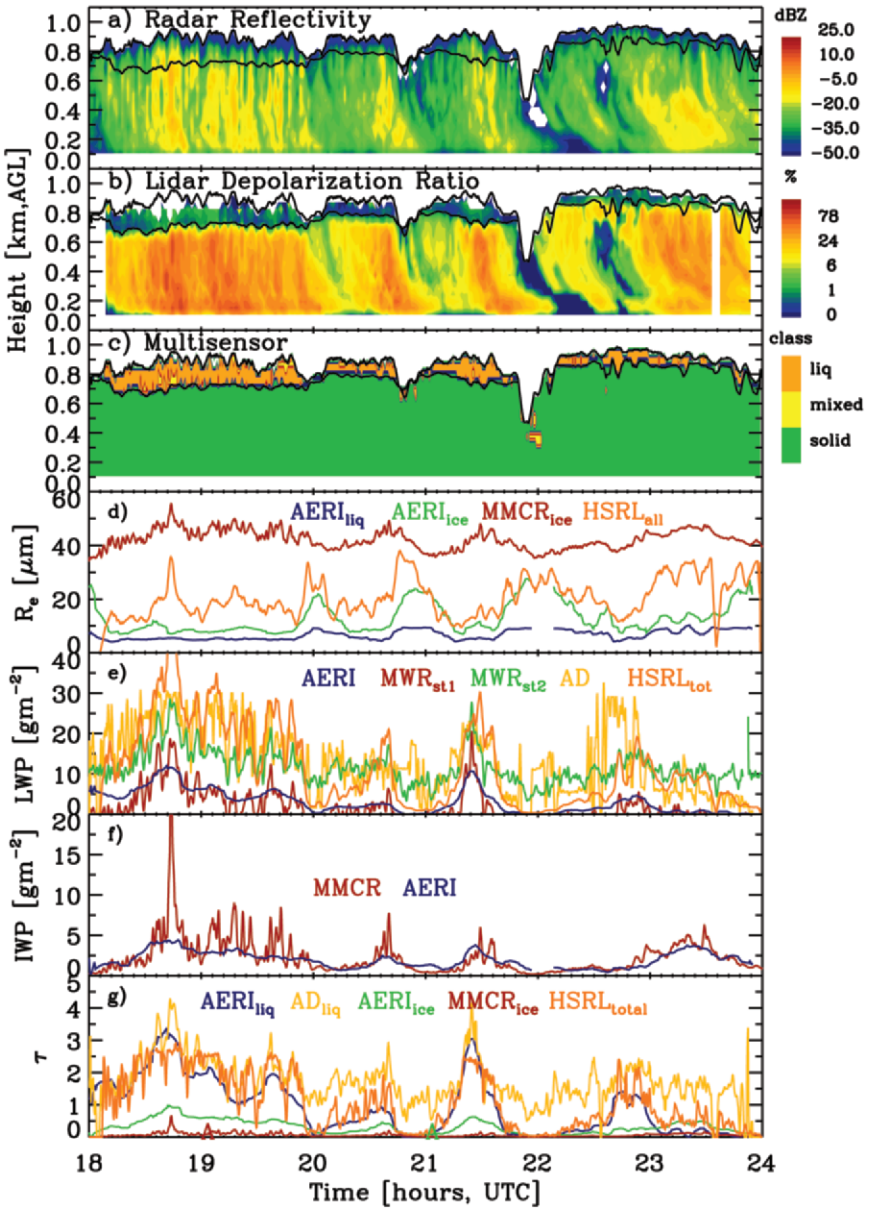

Fig. 4. Measurements and retrievals for 1 Nov 2004 (a) radar reflectivity; (b) lidar depolarization ratio; (c) phase classification derived from the multisensor approach; (d) layer-mean liquid droplet effective radius from AERI, ice particle effective radius from AERI and radar, and a total cloud effective radius from lidar; (e) liquid water path from AERI, microwave radiometer, and an adiabatic assumption, and a total cloud condensed water path from lidar; (f) ice water path from AERI and radar; and (g) optical depth of cloud liquid from AERI and the adiabatic assumption, cloud ice from the AERI and radar, and the total cloud from the lidar. In (a)–(c) the cloud liquid base and top heights, from ceilometer and radar, respectively, are included. The adiabatic optical depth assumes a droplet effective radius of 10 μm.

Cloud liquid microphysics. Vertical profiles of liquid microphysical properties in mixed-phase clouds are more difficult to characterize than ice properties because of limitations in the manner in which different instruments observe the cloud layer. Radar returns are typically dominated by the larger ice crystals, lidar signals often occult near the base of the cloud liquid, and radiometric measurements typically provide only layer-averaged information. There are no robust, widely applicable methods for deriving profiles of liquid droplet effective radius (R_{el}) and only limited possibilities for vertically re-

solving the liquid water content (LWC). The best generalized method for specifying the liquid water profile is a scaled adiabatic LWC assumption, which can be computed using temperature soundings and cloud boundaries identified by radar and lidar (e.g., Zuidema et al. 2005; Illingworth et al. 2007). Because the assumption of adiabatic conditions is not always appropriate, the adiabatic LWC profile is constrained by an independent measure of the LWP to provide a more realistic profile (Fig. 2e).

A number of methods are available to derive LWP (Figs. 3b and 4e). MWR measurements of atmospheric emission near water absorption features in the range of 23–31 GHz are exploited using either statistical or physical iterative approaches (Liljegren et al. 2001; Turner et al. 2007) and are best suited for optically thicker clouds. In addition, differential optical absorption spectroscopy using near-IR measurements provides the cloud LWP during daylight periods (Daniel et al. 2006). For optically thin clouds, IR atmospheric windows are not saturated and contain useful information about cloud liquid properties. AERI measurements in these windows are much more sensitive to thin liquid water layers than the MWR, yielding a more accurate LWP (Turner 2007). Agreement among multiple methods for deriving LWP suggests that this parameter can be obtained with some confidence in thicker clouds. For example, for optically thick clouds (Fig. 3b), standard deviations and biases between the methods are no greater than 35% and 8%, respectively, and correlation coefficients are greater than 0.8. For thinner conditions, the uncertainties associated with deriving LWP from microwave measurements become much higher than from AERI measurements. It is the increased sensitivity of AERI measurements in optically thin conditions that also allows for the only estimate of liquid droplet size, in this case a layer-averaged R_{e1} (Fig. 4d).

Another possible source of cloud liquid water information is radar Doppler spectra. Recent studies (e.g., Shupe et al. 2004; Verlinde et al. 2007; Luke and Kollias 2007) have indicated that under some circumstances, signals from collocated liquid and ice can be separated using Doppler spectra, providing profiles of radar moments for each phase that are used in subsequent microphysics retrievals (Fig. 5). However, in order to accomplish widespread use of this method, sophisticated spectral peak picking, peak separation, and deconvolution methods must be developed.

The combination of both liquid and ice mass information provides an indication of the overall partitioning of condensed phases in mixed-phase clouds. As an example, the liquid fraction (LF), or the ratio of liquid water path to total condensed (liquid plus ice) water path, is given in Fig. 3d. Depending upon which estimates of LWP and IWP are used, the liquid fraction ranges widely; however, in this specific case, there is general agreement on a decreasing trend in time from strong liquid dominance at the beginning to a near balance of liquid and ice mass by the end.

Cloud radiative properties. The extinction coefficient (α) and optical depth (τ) represent an important linkage between clouds and their impact on atmospheric radiation. HSRL observations yield a direct measure of extinction in mixed-phase clouds up to the height of full signal attenuation ($\tau \sim 4$), although extinction at any given level is not distinguished by phase. Ice phase extinction can be derived from radar measurements, under the assumption that the relatively large ice crystals dominate the radar signal, using assumed ice particle mass–area–size and density–size relationships that relate radar reflectivity (proportional to particle size to the sixth power) to extinction (proportional to particle size to the second power; Matrosov et al. 2003). As with liquid microphysical properties, robust methods to derive profiles of liquid extinction through the full depth of optically thick mixed-phase clouds are lacking. The current best estimate for liquid water extinction is to use the scaled adiabatic LWC (e.g., Fig. 2e) combined with an assumed droplet effective radius. Example combined-phase extinction profiles are given in Fig. 2f, which reveal the considerable radiative dominance of cloud liquid water over ice.

From a layer-integrated perspective, multiple optical depth estimates are available (Figs. 3e and 4g) in addition to the vertical integrals of the extinction retrievals. Broadband SW irradiance measurements provide an estimated effective layer optical depth via an empirical expression that incorporates information on sun angle, surface albedo, an equivalent clear-sky SW irradiance, and an assumed asymmetry parameter (Barnard and Long 2004). In this case, it is assumed that all SW obscuration is solely due to the cloud liquid. A near-IR retrieval of LWP, when combined with an assumed liquid droplet radius, also presents an estimate of liquid optical depth (Daniel et al. 2006; Portman et al. 2001). Finally, AERI measurements contain information on both liquid and ice optical depths when radiances are unsaturated (Turner 2005). As in the case of LWP, agreement between methods for liquid optical depth in optically thick clouds (Fig. 3e) is generally quite good, with somewhat less agreement for thinner clouds (Fig. 4g).

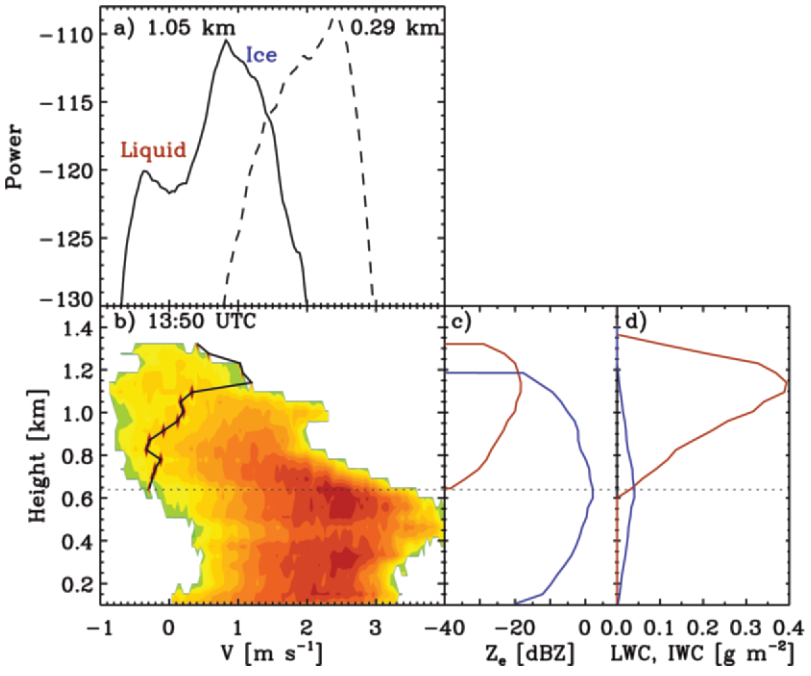

Fig. 5. Doppler radar spectrum analysis at 1350 UTC 9 Oct 2004. The Doppler spectrum is the distribution of returned radar power as a function of the radial velocity of the targets in the radar volume. (a) A bimodal spectrum (solid) found in mixed-phase conditions near cloud top and a unimodal, ice-only spectrum (dashed) found below the liquid cloud base. The ice spectrum has been decreased in power to fit on the same scale as the mixed-phase spectrum. These spectra are horizontal slices through the spectrograph in (b), which shows contours of returned power as a function of velocity and altitude (redder colors indicate higher power). A manually determined line distinguishing the liquid and ice phases has been included, showing a base of the cloud liquid that is in good agreement with the cloud base identified by ceilometer measurements (horizontal dashed line). The location of the liquid spectral peak can be used as a proxy for the vertical air motions since typical liquid cloud droplets are small enough to trace the air motions. Radar velocity measurements are defined as positive toward the radar, or down in this case. (c) Based on the distinction of phase contributions to the spectrograph, individual profiles of liquid and ice reflectivity, which are the total power in each mode, are computed. Apart from the very cloud top, where liquid exists without ice, the ice component strongly dominates the reflectivity. (d) Example profiles of liquid and ice water contents derived from the distinct liquid and ice radar reflectivity profiles are shown. Although the reflectivity is strongly dominated by the ice component (due to larger ice particle sizes), the cloud mass is dominated by liquid water.

Liquid optical depths, shown here, as in many mixed-phase clouds, are 1-2 orders of magnitude larger than those for the ice component.

Cloud dynamical properties. In-cloud dynamics play a key role in shaping the cloud microphysical composition and life cycle. Limited information on in-cloud dynamics can be deduced from ground-based sensors. Under conditions when liquid water is present, vertical wind velocity (W) can be estimated from Doppler radar spectra (Shupe et al. 2008b), based on the assumption that small cloud liquid droplets (~10 μm) act as tracers of vertical air motion. This vertical velocity information, when coupled with Doppler radar velocity measurements, yields cloud ice particle fall speeds. Additionally, the temporal variance of radar mean Doppler velocity provides information on the turbulent dissipation rate (ε, e.g., Bouniol et al. 2003; O'Connor et al. 2005).

Examples of two-dimensional contour maps of retrieved dynamical properties are shown in Figs. 2g,h, while a time series of vertically averaged vertical winds is given in Fig. 3f. Vertical air motion occurs on many time/space scales, suggesting a variety of scales of motion in action in these stratiform Arctic mixed-phase clouds. Spectral analysis of time series data reveals vertical wind variability that is related to cloud-scale (hundreds of meters) up to mesoscale (tens of kilometers) motion (Shupe et al. 2008a).

WHAT HAVE WE LEARNED? The preceding summary details those mixed-phase cloud properties for which some ground-based estimate is available. While it is promising to have at least limited information on this long list of properties, the accuracy with which the retrievals perform varies greatly with instrument and analysis method. Retrieval uncertainties also depend upon the specific conditions and structure of mixed-phase cloudiness. Thus, we make no attempt here to provide definitive uncertainties on any of these methods, but instead defer such matters to the individual references for each method, which also provide the conditions under which the methods perform robustly.

In spite of retrieval uncertainties, there are a number of conclusions that have been drawn from

combinations of ground-based retrievals toward understanding the fundamental composition of mixed-phase clouds and the important processes responsible for their formation and maintenance. These conclusions stand to both confirm and build upon the existing understanding of mixed-phase clouds that has been gained through in situ observations and model analyses.

For example, ground-based observations at many locations have shown supercooled liquid water to occur in discrete layers that are often at the top of, or embedded within, a layer of ice crystals (e.g., Platt 1977; Hogan et al. 2003a; Wang et al. 2004; Zuidema et al. 2005). In single-layer clouds, profiles of ice properties depict the growth of ice crystal size and water content as the ice particles fall through the liquid cloud layer, and the steady ice sublimation as ice crystals fall below the cloud liquid (e.g., Shupe et al. 2006, 2008a). Ice particle retrievals suggest both high temporal variability in ice particle size and concentration (Wang et al. 2004) and differences in particle size and shape between ice-only and mixed-phase clouds (Hogan et al. 2002; Turner 2005). In some cases, observations show ice enhancement resulting from rime-splintering processes associated with liquid layers (Hogan et al. 2002). The riming of liquid water onto ice particles is also indicated by higher ice particle fall speeds than would typically be observed for pristine ice crystals (Shupe et al. 2008a). These observations reveal that ice crystal formation and growth in mixed-phase clouds clearly occurs through mechanisms that involve, or are supported by, the presence of liquid water.

The existing measurements unequivocally reveal the strong radiative dominance of cloud liquid over ice in these cloud layers (Hogan et al. 2003a; Shupe and Intrieri 2004; Turner 2005; Zuidema et al. 2005). This dominance is primarily due to typical background concentrations of cloud condensation nuclei and ice-forming nuclei (IN), which lead to liquid droplets that occur in much higher concentrations and therefore smaller sizes than ice crystals for a given condensed mass. This radiative disparity highlights the importance of properly describing and understanding the mechanisms behind cloud phase partitioning. Proper phase specification is particularly relevant for computing radiative heating rate profiles and for validating model simulations of cloud fields. Observations have shown that the typical partitioning of phase based on temperature alone is likely insufficient (Turner 2005; Shupe et al. 2006).

Recent work has addressed the linkages between cloud microphysical and dynamical properties. Zuidema et al. (2005) observed optically and geometrically thicker clouds under conditions of large-scale lifting and thinner clouds under large-scale subsidence, suggesting the influence of the synoptic scale on local cloud structure. At smaller scales, Shupe et al. (2008a) developed a conceptual model detailing the cycle through which autumn Arctic coastal mixed-phase stratocumulus gain and lose condensate of each phase in response to cloud-scale updrafts. This work revealed the coordinated growth of both phases during shallow mesoscale updrafts, as well as the importance of limited ice concentrations and particle fallout to the maintenance of liquid water. Hogan et al. (2002) also highlighted the impact of narrow updrafts on the formation of liquid water layers and ice particle concentrations in frontal mixed-phase clouds. These dynamical–microphysical linkages ultimately define the cloud phase partitioning that specifies the cloud radiative properties; these, in turn, feed back into driving the cloud-scale circulations.

ADDRESSING THE DEFICIENCIES. There are a number of mixed-phase cloud properties that are clearly not well characterized using current ground-based instruments and methods. These gaps in our observational abilities often confound our understanding of important mixed-phase cloud processes and continue to hinder cloud and atmosphere modeling efforts. We identify the key deficiencies here and offer a number of pathways toward advancing the ground-based characterization of mixed-phase clouds.

One of the most important failures of the current methods, particularly when considered from the cloud radiation perspective, concerns the full vertical characterization of the cloud liquid component. There are presently no widely applicable methods to provide vertical profiles of liquid microphysics or extinction, and under optically thick conditions there is no robust, generally available estimate of even a layer-averaged liquid droplet radius.

A more complete and robust characterization of liquid water properties in mixed-phase clouds might be addressed in a number of ways. Recent investigations using cloud Doppler radar spectra have suggested the possibility of characterizing the liquid component (Shupe et al. 2004; Verlinde et al. 2007; Luke and Kollias 2007), but have been limited to only a few cases. More sophisticated methods, which consider a wider range of spectral features and possibly spectral depolarization ratio, may expose a broader application of Doppler spectra toward

characterizing the liquid phase. The addition of permanent, robust HSRL measurements at the NSA, and other sites, would aid in long-term mixed-phase cloud observations. Combinations of near-IR and visible radiance observations might also be further exploited to derive liquid droplet size information in mixed-phase clouds under daylight conditions (Schofield et al. 2007). Finally, the incorporation of higher-frequency microwave channels may improve the accuracy of LWP retrievals for optically thin conditions (e.g., Crewell and Löhnert 2003); however, these higher frequencies have other issues that will need to be investigated and addressed (e.g., scattering effects, temperature dependence of the dielectric constants, etc.).

An additional and necessary step toward improved microphysical characterization is to reinforce our current retrievals through more extensive validation using in situ observations and multimethod intercomparisons (e.g., Turner and Eloranta 2008). In the near future there are opportunities to support this cause; during the year of 2008 alone there are three aircraft missions scheduled near Barrow, Alaska, and another operated out of the Scandinavian Arctic. One focus of these aircraft missions is validation of ground-based observations and retrievals. In addition, a major effort is under way within the ARM Program to compute radiative heating rate profiles, which are intimately tied to clouds and their properties. Radiative closure experiments, wherein fluxes at the surface and top of the atmosphere are computed from retrieved cloud properties and compared to measurements, provide a metric for cloud property retrieval accuracy (e.g., Turner 2007).

Additionally, little is known about the relationship between aerosol properties and cloud microphysics, phase partitioning, and life cycle. While observations of some near-surface aerosol properties are available, the temporal evolution of aerosol that is accessible by the cloud, either from below or above, is infrequently measured. The combination of relatively scant information on both liquid droplets and aerosol properties in mixed-phase cloud conditions presents a substantial challenge for understanding the aerosol indirect effects on mixed-phase cloudiness.

Details regarding IN and the manner in which ice forms and grows in mixed-phase conditions are unclear and inhibit a better understanding of the cloud life cycle. IN play a key role in these clouds (Pinto 1998; Jiang et al. 2000; Prenni et al. 2007), yet there are no ground-based remote-sensing methods, and few in situ techniques, for measuring IN concentration and type. It is of great interest to understand the temporal variability in IN in order to discern if temporal and spatial patchiness of ice crystals is due to similar variability in IN concentrations or activation. Finally, the ice crystal habit in mixed-phase clouds is also poorly understood because of difficulties in distinguishing crystal habit from ground-based observations, yet it is an important assumption in many retrieval methods and can strongly affect the relationship between ice mass and radiative effects.

Questions regarding ice crystal habit and, by association, the ice crystal growth regime, may be addressed using scanning polarimetric radar and possibly lidar in certain clouds. Short-term studies have highlighted the ability to differentiate a variety of pristine crystal habits as well as rimed particles, aggregates, and graupel (e.g., Matrosov et al. 2001; Reinking et al. 2002) using radar elevation scans. Hogan et al. (2002) utilized differential reflectivity from scanning radar to identify numerous pockets of distinct particle phases within a frontal mixed-phase cloud, allowing for a detailed description of rapid ice formation. Additional focused measurements with high-sensitivity scanning cloud radars are expected to further advance our understanding of ice crystal habit in mixed-phase clouds.

For some variables and processes, such as detailed cloud–aerosol interactions, IN concentrations, and cloud spatial variability, current ground-based measurements are not, and may never be, sufficient. Answers to these questions may require different approaches all together, such as from the perspectives of in situ aircraft observations, satellite measurements, and model analyses. For example, aircraft observations are better suited to make direct measurements of aerosol and cloud properties and can capture a quasi-instantaneous horizontal snapshot of a cloud layer. Satellites provide a much-needed spatial, or global, perspective that is not possible from individual ground stations or aircraft campaigns. Models offer a framework with which to test and examine hypotheses in great detail. While unable to answer all questions regarding mixed-phase clouds, ground-based observations are able to provide instantaneous, high-resolution profiles of many key properties, build continuous long-term statistical data records, and capture temporal variability at many scales. Clearly, the synergy of these perspectives is needed to further cultivate our understanding of mixed-phase clouds.

ACKNOWLEDGMENTS. This research was supported by the Office of Science (BER), U.S. Department of Energy. Thanks to the ARM Program and MPACE team for collecting a well-focused mixed-phase cloud dataset.

REFERENCES

Ackerman, T. P., and G. Stokes, 2003: The Atmospheric Radiation Measurement Program. *Phys. Today,* **56,** 38–45.

Barnard, J. C., and C. N. Long, 2004: A simple empirical equation to calculate cloud optical thickness using shortwave broadband measurements. *J. Appl. Meteor.,* **43,** 1057–1066.

Bouniol, D., A. J. Illingworth, and R. J. Hogan, 2003: Deriving turbulent kinetic energy dissipation rate within clouds using ground based 94 GHz radar. Preprints, *31st Conf. on Radar Meteorology,* Seattle, WA, Amer. Meteor. Soc. 4A.5. [Available online at http://ams.confex.com/ams/pdfpapers/63826.pdf.]

Campbell, J. R., D. L. Hlavka, E. J. Welton, C. J. Flynn, D. D. Turner, J. D. Spinhirne, and V. S. Scott, 2002: Full-time eye-safe cloud and aerosol lidar observations at atmospheric radiation measurement program sites: Instruments and data processing. *J. Atmos. Oceanic Technol.,* **19,** 431–442.

Clothiaux, E. E., T. P. Ackerman, G. G. Mace, K. P. Moran, R. T. Marchand, M. A. Miller, and B. E. Martner, 2000: Objective determination of cloud heights and radar reflectivities using a combination of active remote sensors at the ARM CART sites. *J. Appl. Meteor.,* **39,** 645–665.

Cober, S. G., G. A. Isaac, and J. W. Strapp, 2001: Characterizations of aircraft icing environments that include supercooled large drops. *J. Appl. Meteor.,* **40,** 1984–2002.

Crewell, S., and U. Löhnert, 2003: Accuracy of cloud liquid water path from ground-based microwave radiometer 2. Sensor accuracy and synergy. *Radio Sci.,* **38,** 8042, doi:10.1029/2002RS002634.

Daniel, J. S., and Coauthors, 2006: Cloud property estimates from zenith spectral measurements of scattered sunlight between 0.9 and 1.7 μm. *J. Geophys. Res.,* **111,** D16208, doi:10.1029/2005JD006641.

Donovan, D. P., and A. C. A. P. van Lammeren, 2001: Cloud effective particle size and water content profile retrievals using combined lidar and radar observations 1. Theory and examples. *J. Geophys. Res.,* **106,** 27 425–27 448.

Eloranta, E. W., 2005: High spectral resolution lidar. *Lidar: Range-Resolved Optical Remote Sensing of the Atmosphere,* K. Weitkamp, Ed., Springer-Verlag 143–163.

Field, P. R., R. J. Hogan, P. R. A. Brown, A. J. Illingworth, R. W. Choularton, P. H. Kaye, E. Hirst, and R. Greenaway, 2004: Simultaneous radar and aircraft observations of mixed-phase cloud at the 100 m scale. *Quart. J. Roy. Meteor. Soc.,* **130,** 1877–1904.

Fleishauer, R. P., V. E. Larson, and T. H. Vonder Haar, 2002: Observed microphysical structure of midlevel, mixed-phase clouds. *J. Atmos. Sci.,* **59,** 1779–1804.

Gayet, J.-F., S. Asano, A. Yamazaki, A. Uchiyama, A. Sinyuk, O. Jourdan, and F. Auriol, 2002: Two case studies of winter continental-type water and mixed-phase stratocumuli over the sea 1. Microphysical and optical properties. *J. Geophys. Res.,* **107,** 4569, doi:10.1029/2001JD001106.

Gregory, D., and D. Morris, 1996: The sensitivity of climate simulations to the specification of mixed phase clouds. *Climate Dyn.,* **12,** 641–651.

Haeffelin, M., and Coauthors, 2005: SIRTA, a ground-based atmospheric observatory for cloud and aerosol research. *Ann. Geophys.,* **23,** 253–275.

Heymsfield, A. J., and L. M. Miloshevich, 1993: Homogeneous ice nucleation and supercooled liquid water in orographic wave clouds. *J. Atmos. Sci.,* **50,** 2235–2353.

——, ——, A. Slingo, K. Sassen, and D. O'C. Starr, 1991: An observational and theoretical study of highly supercooled altocumulus. *J. Atmos. Sci.,* **48,** 923–945.

Hobbs, P. V., and D. G. Atkinson, 1976: The concentrations of ice particles in orographic clouds and cyclonic storms over the Cascade Mountains. *J. Atmos. Sci.,* **33,** 1362–1374.

——, and A. L. Rangno, 1998: Microstructures of low and middle-level clouds over the Beaufort Sea. *Quart. J. Roy. Meteor. Soc.,* **124,** 2035–2071.

Hogan, R. J., P. R. Field, A. J. Illingworth, R. J. Cotton, and T. W. Choularton, 2002: Properties of embedded convection in warm-frontal mixed-phase cloud from aircraft and polarimetric radar. *Quart. J. Roy. Meteor. Soc.,* **128,** 451–476.

——, P. N. Francis, H. Flentje, A. J. Illingworth, M. Quante, and J. Pelon, 2003a: Characteristics of mixed-phase clouds. I: Lidar, radar and aircraft observations from CLARE '98. *Quart. J. Roy. Meteor. Soc.,* **129,** 2089–2116.

——, A. J. Illingworth, E. J. O'Connor, and J. P. V. Poiares Baptista, 2003b: Characteristics of mixed-phase clouds, Part II: A climatology from ground-based lidar. *Quart. J. Roy. Meteor. Soc.,* **129,** 2117–2134.

——, M. P. Mittermaier, and A. J. Illingworth, 2006: The retrieval of ice water content from radar reflectivity factor and termperature and its use in evaluating a mesoscale model. *J. Appl. Meteor. Climatol.,* **45,** 301–317.

Illingworth, A. J. and Coauthors, 2007: CloudNet: Continuous evaluations of cloud profiles in seven operational models using ground-based observations. *Bull. Amer. Meteor. Soc.,* **88,** 883–898.

Jiange, H., W. R. Cotton, J. O. Pinto, J. A. Curry, and M. J. Weissbluth, 2000: Cloud resolving simulations of mixed-phase Arctic stratus observed during BASE: Sensitivity to concentration of ice crystals and large-scale heat and moisture advection. *J. Atmos. Sci.,* **57,** 2105–2117.

Knuteson, R. O., and Coauthors, 2004a: Atmospheric Emitted Radiance Interferometer. Part I: Instrument design. *J. Atmos. Oceanic Technol.,* **21,** 1763–1776.

——, and Coauthors, 2004b: Atmospheric Emitted Radiance Interferometer. Part I: Instrument performance. *J. Atmos. Oceanic Technol.,* **21,** 1777–1789.

Kollias, P., E. E. Clothiaux, M. A. Miller, E. Luke, K. L. Johnson, K. P. Moran, K. B. Widener, and B. A. Albrecht, 2007: The Atmospheric Radiation Measurement Program cloud profiling radars: Second generation sampling strategies, processing, and cloud data products. *J. Atmos. Oceanic Technol.,* **24,** 1199–1214.

Korolev, A. V., G. A. Isaac, S. G. Cober, J. W. Strapp, and J. Hallett, 2003: Microphysical characterization of mixed-phase clouds. *Quart. J. Roy. Meteor. Soc.,* **129,** 39–65.

Liljegren, J. C., 1994: Two-channel microwave radiometer for observations of total column precipitable water vapor and cloud liquid water path. Preprints, *Fifth Symp. on Global Change Studies,* Nashville, TN, Amer. Meteor. Soc., 262–269.

——, E. E. Clothiaux, G. G. Mace, S. Kato, and X. Dong, 2001: A new retrieval for cloud liquid water path using a ground-based microwave radiometer and measurements of cloud temperature. *J. Geophys. Res.,* **106,** 14 485–14 500.

Lubin, D., 2004: Thermodynamic phase of maritime Antarctic clouds from FTIR and supplementary radiometric data. *J. Geophys. Res.,* **109,** D04204, doi:10.1029/2003JD003979.

Luke, E., and P. Kollias, 2007: A high resolution hydrometeor phase classifier based on analysis of cloud radar Doppler spectra. *Proc. of the 33rd Conf. on Radar Meteorology,* Cairns, Australia, Amer. Meteor. Soc., 6A.2. [Available online at http://ams.confex.com/ams/pdfpapers/123629.pdf.]

Mace, G. G., A. J. Heymsfield, and M. R. Poellot, 2002: On retrieving the microphysical properties of cirrus clouds using the moments of the millimeter-wavelength Doppler spectrum. *J. Geophys. Res.,* **107,** 4815, doi:10.1029/2001JD001308.

Matejka, T. J., R. A. Houze Jr., and P. V. Hobbs, 1980: Microphysics and dynamics of clouds associated with mesoscale rainbands in extratropical cyclones. *Quart. J. Roy. Meteor. Soc.,* **106,** 29–56.

Matrosov, S. Y., R. F. Reinking, R. A. Kropfli, B. E. Martner, and B. W. Bartram, 2001: On the use of radar depolarization ratios for estimating shapes of ice hydrometeors in winter clouds. *J. Appl. Meteor.,* **40,** 479–490.

——, A. V. Korolev, and A. J. Heymsfield, 2002: Profiling cloud mass and particle characteristic size from Doppler radar measurements. *J. Atmos. Oceanic Technol.,* **19,** 1003–1018.

——, M. D. Shupe, A. J. Heymsfield, and P. Zuidema, 2003: Ice cloud optical thickness and extinction estimates from radar measurements. *J. Appl. Meteor.,* **42,** 1584–1597.

Moran, K. P., B. E. Martner, M. J. Post, R. A. Kropfli, D. C. Welsh, and K. B. Widener, 1998: An unattended cloud-profiling radar for use in climate research. *Bull. Amer. Meteor. Soc.,* **79,** 443–455.

O'Connor, E. J., R. J. Hogan, and A. J. Illingworth, 2005: Retrieving stratocumulus drizzle parameters using Doppler radar and lidar. *J. Appl. Meteor.,* **44,** 14–27.

Pinto, J. O., 1998: Autumnal mixed-phase cloudy boundary layers in the Arctic. *J. Atmos. Sci.,* **55,** 2016–2038.

Platt, C. M. R., 1977: Lidar observations of a mixed-phase altostratus cloud. *J. Appl. Meteor.,* **16,** 339–345.

Portmann, R. W., S. Solomon, R. W. Sanders, J. S. Daniel, and E. G. Dutton, 2001: Cloud modulation of zenith sky oxygen photon path lengths over Boulder, Colorado: Measurements versus model. *J. Geophys. Res.,* **106,** 1139–1155.

Prenni, A. J., and Coauthors, 2007: Can ice-nucleating aerosols affect Arctic seasonal climate? *Bull. Amer. Meteor. Soc.,* **88,** 541–550.

Pruppacher, H. R., and J. D. Klett, 1978: *Microphysics of Clouds and Precipitation.* D. Reidel, 454 pp.

Rangno, A. L., and P. V. Hobbs, 1991: Ice particle concentrations and precipitation development in small polar maritime cumuliform clouds. *Quart. J. Roy. Meteor. Soc.,* **117,** 207–241.

Rauber, R. M., 1987: Characteristics of cloud ice and precipitation during wintertime storms over the mountains of Northern Colorado. *J. Climate Appl. Meteor.,* **26,** 488–524.

Reinking, R. F., S. Y. Matrosov, R. A. Kropfli, and B. W. Bartram, 2002: Evaluation of a 45° slant quasi-linear radar polarization state for distinguishing drizzle droplets, pristine ice crystals, and less regular ice particles. *J. Atmos. Oceanic Technol.,* **19,** 296–321.

Schofield, R., and Coauthors, 2007: Retrieval of effective radius and liquid water path from ground-based instruments: A case study at Barrow, Alaska. *J. Geophys. Res.,* **112,** D21203, doi:10.1029/2007JD008737.

Shupe, M. D., 2007: A ground-based multisensor cloud phase classifier. *Geophys. Res. Lett.,* **34,** L22809, doi:10.1029/2007GL031008.

——, and J. M. Intrieri, 2004: Cloud radiative forcing of the Arctic surface: The influence of cloud properties, surface albedo, and solar zenith angle, *J. Climate,* **17,** 616–628.

——, P. Kollias, S. Y. Matrosov, and T. L. Schnieder, 2004: Deriving mixed-phase cloud properties from Doppler radar spectra. *J. Atmos. Oceanic Technol.,* **21,** 660–670.

——, T. Uttal, and S. Y. Matrosov, 2005: Arctic cloud microphysics retrievals from surface-based remote sensors at SHEBA. *J. Appl. Meteor.,* **44,** 1544–1562.

——, S. Y. Matrosov, and T. Uttal, 2006: Arctic mixed-phase cloud properties derived from surface-based sensors at SHEBA. *J. Atmos. Sci.,* **63,** 697–711.

——, P. Kollias, P. O. G. Persson, and G. M. McFarquhar, 2008a: Vertical motions in Arctic mixed-phase stratus. *J. Atmos. Sci.,* **65,** 1304–1322.

——, ——, M. Poellot, and E. Eloranta, 2008b: On deriving vertical air motions from cloud radar Doppler spectra. *J. Atmos. Oceanic Technol.,* **25,** 547–557.

Sun, Z., and K. P. Shine, 1994: Studies of the radiative properties of ice and mixed-phase clouds. *Quart. J. Roy. Meteor. Soc.,* **120,** 111–137.

Turner, D. D., 2005: Arctic mixed-phase cloud properties from AERI lidar observations: Algorithm and results from SHEBA. *J. Appl. Meteor.,* **44,** 427–444.

——, 2007: Improved ground-based liquid water path retrievals using a combined infrared and microwave approach. *J. Geophys. Res.,* **112,** D15204, doi:10.1029/2007JD008530.

——, and R. E. Holz, 2005: Retrieving cloud fraction in the field-of-view of a high-spectral-resolution infrared radiometer. *IEEE Geosci. Remote Sens. Lett.,* **3,** 287–291.

——, and E. Eloranta, 2008: Validating mixed-phase cloud optical depth retrieved from infrared observations with high spectral resolution lidar. *IEEE Geosci. Remote Sens. Lett.,* **5,** 285–288.

——, S. A. Clough, J. C. Liljegren, E. E. Clothiaux, K. Cady-Pereira, and K. L. Gaustad, 2007: Retrieving liquid water path and precipitable water vapor from the Atmospheric Radiation Measurement (ARM) microwave radiometers. *IEEE Trans. Geosci. Remote Sens.,* **45,** 3680–3690.

Verlinde, H., and Coauthors, 2007: The Mixed-Phase Arctic Cloud Experiment (M-PACE). *Bull. Amer. Meteor. Soc.,* **88,** 205–221.

Wang, Z., and K. Sassen, 2002: Cirrus cloud microphysical property retrieval using lidar and radar measurements. Part I: Algorithm description and comparison with in situ data. *J. App. Meteor.,* **41,** 218–229.

——, ——, D. N. Whiteman, and B. B. Demoz, 2004: Studying altocumulus with ice virga using ground-based active and passive remote sensors. *J. Appl. Meteor.,* **43,** 449–460.

Zuidema, P., and Coauthors, 2005: An Arctic springtime mixed-phase cloudy boundary layer observed during SHEBA. *J. Atmos. Sci.,* **62,** 160–176.